

Surface mass balance, thinning and iceberg production, Columbia Glacier, Alaska, 1948–2007

L.A. RASMUSSEN,¹ H. CONWAY,¹ R.M. KRIMMEL,² R. HOCK^{3,4}

¹Department of Earth and Space Sciences, University of Washington, Box 351310, Seattle, Washington 98195-1310, USA
E-mail: lar@ess.washington.edu

²14542 SW Pohl Road, Vashon, Washington 98070, USA

³Geophysical Institute, University of Alaska Fairbanks, PO Box 757320, Fairbanks, Alaska 99775-7320, USA

⁴Department of Earth Sciences, Uppsala University, Villavägen 16, SE-752 36 Uppsala, Sweden

ABSTRACT. A mass-balance model using upper-air meteorological data for input was calibrated with surface mass balance measured mainly during 1977–78 at 67 sites on Columbia Glacier, Alaska, between 135 and 2645 m a.s.l. Root-mean-square error, model vs measured, is $1.0 \text{ m w.e. a}^{-1}$, with $r^2 = 0.88$. A remarkable result of the analysis was that both precipitation and the factor in the positive degree-day model used to estimate surface ablation were constant with altitude. The model was applied to reconstruct glacier-wide components of surface mass balance over 1948–2007. Surface ablation, $4 \text{ km}^3 \text{ ice eq. a}^{-1}$ (ice equivalent), has changed little throughout the period. From 1948 until about 1981, when drastic retreat began, the surface mass balance was positive but changes in glacier geometry were small, so the positive balance was offset by calving, $\sim 0.9 \text{ km}^3 \text{ ice eq. a}^{-1}$. During retreat, volume loss of the glacier accounted for 92% of the iceberg production. Calving increased to $\sim 4.3 \text{ km}^3 \text{ ice eq. a}^{-1}$ from 1982 to 1995, and after that until 2007 to $\sim 8.0 \text{ km}^3 \text{ ice eq. a}^{-1}$, which was about twice the loss by surface ablation, whereas prior to retreat it was only about a quarter as much. Calving is calculated as the difference between glacier-wide surface mass balance and geodetically determined volume change.

INTRODUCTION

Rise of sea level caused by increased discharge of ice from the world's glaciers, ice caps and ice sheets would have numerous profound economic and social consequences (Schneider and others, 2007). The fate of land-based ice depends on future climate and dynamics of outlet glaciers terminating in the sea. Climate variations have immediate effects on the glacier surface, but effects on the overall behavior of outlet glaciers that are cumulative over decades or centuries are poorly understood.

Shrinkage of southeastern Alaska glaciers accounts for $\sim 20\%$ of the total contribution of glaciers, ice caps and ice sheets to sea-level rise (Meier and others, 2007). Recent volume changes of several glaciers in the region (including Columbia Glacier) have been determined by laser altimetry (Arendt and others, 2002). Berthier and others (2010) compared recent satellite imagery with earlier digital elevation models constructed by the US Geological Survey (USGS) and determined that mass loss of Columbia Glacier over ~ 1960 –2006 was $\sim 6\%$ of the total loss of Alaska glaciers. These studies of mass loss do not separately resolve effects of surface mass balance and mass loss by calving.

The extensive observational record at Columbia Glacier, and previous analysis of it, is an invaluable resource for investigating the behavior of such ocean-terminating glaciers. The major part of this record is the series of 139 vertical aerial photography flights between 1957 and June 2010, most of which covered only the $\sim 20 \text{ km}$ long lower reach. Photogrammetric analysis yielded changes between successive flights in horizontal and vertical coordinates of many identifiable surface features (Krimmel, 2001). As noted below, however, there is only a very small body of surface mass-balance measurements.

There is only a small record of 67 direct measurements of surface mass balance on Columbia Glacier in 1977–78

(Mayo and others, 1979), 1983–95 (Krimmel, 2001) and 1992–97. A model of surface mass balance (Rasmussen and Conway, 2004) using an established upper-air database is calibrated here for Columbia Glacier with the 67 measurements.

The model thus calibrated is used to construct the surface mass-balance record over 1948–2007. This paper also estimates the 1948–2007 iceberg production resulting from the combination of surface mass-balance processes and volume loss due to drawdown of the glacier surface, as well as disintegration of the part of the lower reach between the pre-retreat terminus and the 2007 terminus. Projecting possible future dynamic changes in the glacier is not the purpose of this paper. Future surface mass balance, however, is estimated under continuation of climate conditions that existed over 1995–2007 and under postulated changes in temperature and precipitation.

COLUMBIA GLACIER

Columbia Glacier (Fig. 1) is a large temperate glacier flowing from 3700 m a.s.l. on the south side of the Chugach Mountains to a fjord that empties into Prince William Sound. From its first recorded observation in 1794 (Vancouver, 1798) until ~ 1981 , the glacier terminus rested on a marine shoal at about $L = 67 \text{ km}$, where L is the distance from the head of the glacier measured along its main flowline. At that time the glacier area was $\sim 1070 \text{ km}^2$. Calkin and others (2001) found that the advance to that position from at least 10 km up-glacier began as early as the 15th century.

Water depths at the shoal measured in 1973 ranged from < 2 to $\sim 30 \text{ m}$, but behind it the water was several hundred meters deep (Post, 1975). Post correctly surmised that if the terminus retreated into the deeper water, calving would increase beyond the rate of ice flow to the terminus, and

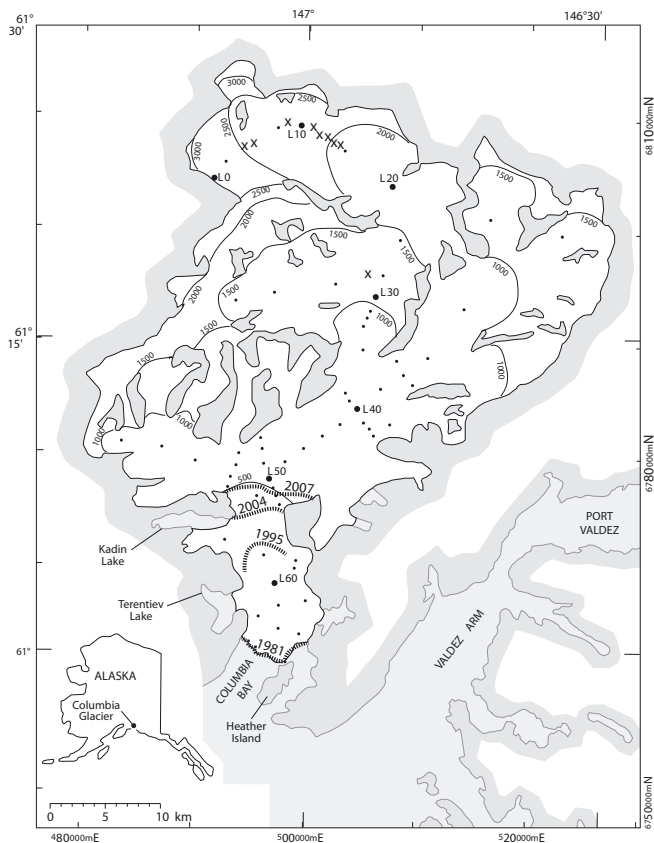


Fig. 1. Columbia Glacier, showing pre-retreat and later terminus positions. Closed circles indicate 1977–78 mass-balance stake measurements. Crosses are crevasse measurements. Open circles indicate distance, L , (km) from the head of the glacier following the main flowline. Universal Transverse Mercator (UTM) coordinates (m) are in zone 6 of the North American Datum of 1927 (NAD27). Contours are for pre-retreat topography (fig. 1 of Mayo and others, 1979). Valdez AP is at 61.3° N, 146.35° W. The nearest NCEP/NCAR point is at 60° N, 147.5° W.

the glacier would undergo drastic retreat. Terminus retreat began slowly in ~ 1981 and accelerated to its maximum rate ($\sim 1 \text{ km a}^{-1}$) 10 years later (Krimmel, 2001). Although the rate of flow to the terminus increased by about an order of magnitude, it could not compensate for the increased calving (Van der Veen, 1995). Ice speed at the terminus increased from $\sim 2 \text{ km a}^{-1}$ in 1981 to $\sim 12 \text{ km a}^{-1}$ in 2001 (Pfeffer, 2007).

By 2004 (O'Neel and others, 2005) the terminus had retreated to $L = 52 \text{ km}$ and by 2010 to $L = 49 \text{ km}$ (Fig. 1). According to radar soundings in 1977 and 1978 (Mayo and others, 1979), the glacier bed is below sea level for another 15 km up-glacier from the 2010 terminus position. Pfeffer (2007) concluded from analysis of the glacier's flow characteristics that retreat will continue.

DATA SOURCES

Surface mass balance

Surface mass-balance measurements were made in late summer 1977 and 1978 on the glacier (Mayo and others, 1979) at 56 locations ranging from 135 to 2645 m a.s.l. They were made by the direct glaciological method of using stakes drilled into the ice. A few other measurements were made indirectly.

On 3 August 1997, D. Trabant and Krimmel measured on crevasse walls the depth from the glacier surface to the ash layer deposited by the 18 August 1992 eruption of Mount Spurr, 260 km to the west. Mean altitude of the sites over the 5 years was determined by taking into account glacier slope and 1992–93 measured flow, resulting in assigning a mean altitude 60 m above that measured in 1997. Mean altitudes of the ten sites range between 944 and 2498 m a.s.l.

Surface lowering was measured photogrammetrically on the occasion of ten vertical aerial photography flights (6 November 1983 to 27 September 1995) at a site on stagnant ice near the terminus (Krimmel, 2001). The rate of lowering was nearly constant over the 12 year period while the surface altitude at the site decreased from ~ 200 to $\sim 100 \text{ m}$. Because the glacier surface there in that season is snow-free, the lowering is due to ice loss, about -9.4 m a^{-1} .

Mass-balance records for Wolverine and Gulkana Glaciers were integrated over their 1966 topography (Van Beusekom and others, 2011) and for South Cascade Glacier over its 1970 topography (Rasmussen, 2009). These USGS programs have been maintained since 1966 at the first two glaciers, and since 1958 at the third.

Glacier geometry

The 1957 area–altitude distribution in 100 ft ($\sim 30.5 \text{ m}$) altitude bands was supplied by S. O'Neel (personal communication, 2009). The 2007 area–altitude distribution in 50 m altitude bands derived from 5 m resolution satellite images (Korona and others, 2009) was supplied by E. Berthier (personal communication, 2010).

Bathymetry of part of the fjord occupied by the glacier prior to retreat was surveyed by the US National Oceanographic and Atmospheric Administration (NOAA) in September 2005. It was supplied south of $L = 51.7 \text{ km}$ (Fig. 1) on a 100 m square grid by S. O'Neel (personal communication, 2009). Bathymetry on a 200 m square grid south of $L = 55.3 \text{ km}$ was constructed (Krimmel, 2001) from surveys by the USGS in late summer or fall over 1995–97. Calving rate over 1981–95 is also given by Krimmel (2001).

Meteorological conditions

US National Centers for Environmental Prediction and US National Center for Atmospheric Research (NCEP/NCAR) Reanalysis data (Kalnay and others, 1996; Kistler and others, 2001) give values of meteorological variables at many levels in the atmosphere at integer multiples of 2.5° in both latitude and longitude. The database has the advantages that it has 6 hour temporal resolution, is free of missing values and is maintained as an integral part of an ongoing major scientific enterprise. The nearest gridpoint (60.0° N, 147.5° W) is 125 km due south of the 2007 glacier terminus. Daily data there at 1200 UTC for 1948–2007 at four standard levels, 1000, 925, 850 and 700 hPa, were downloaded in May 2008 from Columbia University: <http://ingrid.ldgo.columbia.edu/SOURCES/.NOAA/.NCEP-NCAR/.CDAS-1/>.

Daily meteorological observations have been made since summer 1975 at the Valdez US National Weather Service Office (61.13° N, 146.35° W), which is $\sim 35 \text{ km}$ east of the 2007 glacier terminus. Seasonal variation of mean 1948–2007 upper-air conditions is shown in Figure 2, along with mean 1976–2007 Valdez precipitation.

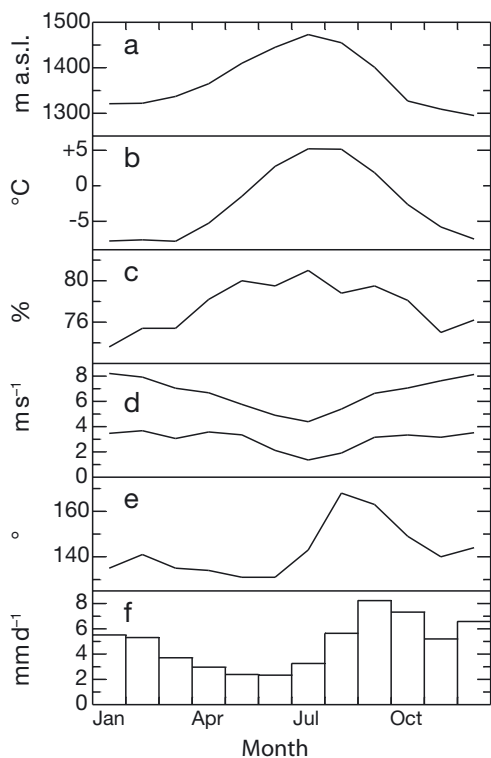


Fig. 2. (a–e) Mean 1948–2007 conditions at 850 hPa at 60° N, 147.5° W: (a) geopotential height, (b) temperature, (c) relative humidity, (d) wind speed (upper) and magnitude of mean vector wind (lower), and (e) direction of mean vector wind. (f) Mean 1976–2007 Valdez precipitation.

SURFACE MASS-BALANCE MODEL

Mass-balance modeling has historically obtained meteorological data either from regular weather service stations for analysis over several years (De Woul and Hock, 2005) or from automated weather stations operated on or near the glacier for analysis over one or a few years (Andreassen and Oerlemans, 2009). Upper-air meteorological data were initially used to model surface accumulation by Rasmussen and Conway (2001) and to model surface ablation by Rasmussen and Conway (2003). They have been used since then to model mass balance in Scandinavia (Rasmussen and Conway, 2005), Iceland (Rasmussen, 2005), Svalbard (Rasmussen and Kohler, 2007) and on Mount Rainier, Washington, USA (Rasmussen and Wenger, 2009).

Surface accumulation

Precipitation, P , is partitioned between rain and snow, c_{sfc} , at any altitude, z , by interpolating temperature, $T(z)$, in the NCEP/NCAR data. Rain, the part of P when $T(z) > +2^\circ\text{C}$, is assumed to run off without refreezing in the glacier. Although other values have been used for the rain/snow transition, including 0°C by some authors, there is abundant support for using $+2^\circ\text{C}$ (Oerlemans, 1991; Førland and Hanssen-Bauer, 2003; Kohler and Aanes, 2004).

Surface accumulation over the period $[t_1, t_2]$ in days is taken to be equal to the snowfall, which is calculated from

$$c_{\text{sfc}}(z) = \alpha \sum_{t_1}^{t_2} f(z), \quad (1)$$

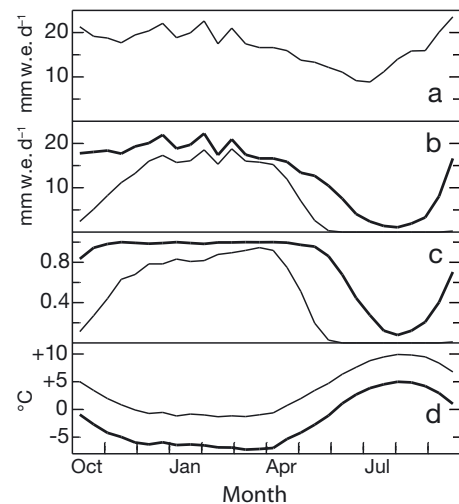


Fig. 3. Model estimates of climatological conditions averaged over 1948–2007. (a) Precipitation, (b) snowfall, (c) snowfall/precipitation ratio and (d) temperature. Heavy curves are for 1000 m a.s.l.; light curves are for 500 m a.s.l.

in which the flux, f , is

$$f(z) = \begin{cases} P & T(z) \leq +2^\circ\text{C} \\ 0 & T(z) > +2^\circ\text{C} \end{cases} \quad (2)$$

and pseudo-precipitation $P = \max[0, \text{RH } U(\phi')]$. Here $0 \leq \text{RH} \leq 1$ is the 850 hPa relative humidity and U is the component of the wind from critical direction ϕ' . That is, $U = |\vec{V}_{850}| \cos(\phi_{850} - \phi')$, in which $|\vec{V}_{850}|$ is the speed and ϕ_{850} the direction of the 850 hPa wind. Because RH is dimensionless, f has the same units as U (m s^{-1}). The proportionality coefficient, α , and critical direction, ϕ' , are two of the three parameters of the model.

Mean 1948–2007 seasonal variation of calculated climatological conditions is shown in Figure 3 for 500 and 1000 m a.s.l. The snow fraction, c_{sfc}/P , at 1000 m is uniformly high from mid-fall through late spring. At 500 m the fraction slowly increases from a low value early in that period and approaches the 1000 m value only at the end of it, even though T is comparable at the beginning and end. The cause is a peculiarity of the $T(t, z)$ distribution: there are relatively more days with $T \geq +2^\circ\text{C}$ at 500 m early in the winter than late, but not at 1000 m.

Model precipitation has about the same general seasonal variation as measured precipitation (Fig. 2) at Valdez, i.e. with a spring minimum, but has much greater amplitude. This is due in part to Valdez station being at the head of the fjord (Port Valdez; Fig. 1) and thus being partially shielded, by high topography, from storms from the south.

Surface ablation

A one-coefficient degree-day model is used to estimate ablation:

$$a_{\text{sfc}}(z) = -\beta \sum_{t_1}^{t_2} T^+(z), \quad (3)$$

in which $T^+ = \max(0, T)$ and t_1 and t_2 are as in Equation (1). Temperature, T , is interpolated at z in the reanalysis data, and β is the third model parameter, along with α and ϕ' in Equations (1) and (2).

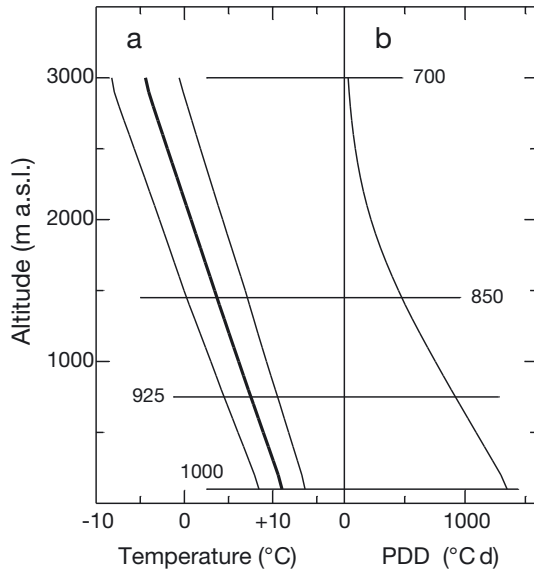


Fig. 4. Mean June–September vertical profiles of temperature at 60.0° N, 147.5° W over 1948–2007. (a) \bar{T} (heavy) and $\bar{T} \pm \sigma$ (light); (b) positive degree-days (PDD) $\sum T^+$. Mean summer altitudes of the 1000, 925, 850 and 700 hPa levels are shown; in winter they are lower, from $\sim 50\%$ at 1000 hPa to $\sim 10\%$ at 700 hPa.

The mean 1948–2007 June–September vertical profile of the T^+ sum is shown in Figure 4, along with that of $\bar{T} \pm \sigma_T$.

Annual surface balance

Surface mass balance is the sum of surface accumulation and surface ablation:

$$b_{\text{sfc}}(z) = c_{\text{sfc}}(z) + a_{\text{sfc}}(z), \quad (4)$$

in which c_{sfc} is given by Equations (1) and (2) and a_{sfc} by Equation (3). Because the surface mass-balance measurements span such a large altitude range, there is good resolution of the coefficients α and β . Observations at high (low) altitude pertain mainly to the α (β) term. Conversely, if the measurements had all been at similar altitudes, the resolution would have been poor; i.e. Equation (4) would approach being one equation with two unknowns, α and β . That is, an infinite number of $c_{\text{sfc}}, a_{\text{sfc}}$ pairs, and underlying α, β pairs, would satisfy Equation (4).

Temperature in the upper-air database is at 1200 UTC (about 0200 local time), which means T^+ is taken from near the minimum of the diurnal cycle. Thus coefficient β is numerically larger than it would be were T^+ taken near the maximum of the cycle. That is, β and the T^+ sum are inversely related because their product (Equation (3)) is controlled by the measured surface balance, \hat{b}_{sfc} , at low altitude. Amplitude of the diurnal cycle is small in the upper air, so this effect is probably also small.

Model results

Coefficients optimized by minimizing the root-mean-square (rms) error between measured and modeled values using the 67 mass-balance measurements over 1977–97 are $\alpha = 0.0061$ s and $\beta = 0.0041$ m d $^{-1}$ °C $^{-1}$ with $\phi' = 200^\circ$. The β value is typical for a snow-covered surface, which is the case on Columbia Glacier for much of the year. In comparing the model results with measurements, t_1 and t_2 in Equations (1) and (3) are the dates of the measurements. In calculating

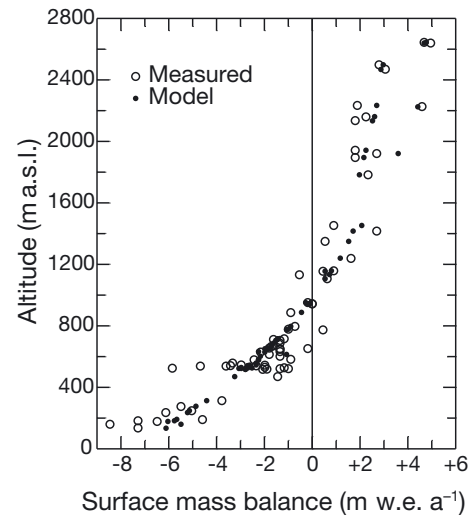


Fig. 5. Surface mass balance: measured (\hat{b}_{sfc}) and model (b_{sfc}) estimates ($n = 67$). (Details are given in the Data sources section.)

balances over other periods, t_1 and t_2 are chosen to span the entire year. Results are weakly sensitive to model parameter ϕ' because of the slow variation of the cosine factor in the expression for U in forming P in Equation (2).

Goodness of fit of the model is expressed by the rms of the model errors, $b_{\text{sfc}}(z) - \hat{b}_{\text{sfc}}(z)$, and by the coefficient of determination (Bevington, 1969):

$$r^2 = 1 - \left(\frac{\text{rms}}{\sigma} \right)^2, \quad (5)$$

in which σ is the standard deviation of $\hat{b}_{\text{sfc}}(z)$. The rms model error over the 67 cases is 1.0 m w.e. a $^{-1}$ with $r^2 = 0.88$ (Fig. 5).

Inclusion of a constant term in Equation (4) produces negligible improvement. Although the model makes the unusual assumptions that neither precipitation, P (Equation (2)), nor the degree-day coefficient, β (Equation (3)), varies with altitude, model error is uncorrelated with altitude ($r = +0.05$). Because there is no constant term in Equation (4), the mean error is not necessarily zero; in the results here it is $+0.03$ m w.e. Mean 1948–2007 vertical profiles of calculated surface accumulation, c_{sfc} , surface ablation, a_{sfc} , and surface mass balance, b_{sfc} , are shown in Figure 6.

An implicit assumption of the model is that surface mass-balance components do not vary along an altitude contour. The measurements vary principally with altitude but there is a slight secondary variation, such as in the annual values at ~ 500 m (Fig. 5). Inability to capture lateral variation is a source of much model error. When integrated over the topography, however, much of this error component cancels out. Although the error is large at any particular site (1.0 m w.e. a $^{-1}$), errors, $b_{\text{sfc}} - \hat{b}_{\text{sfc}}$, at individual sites tend to cancel each other when averaged over the entire glacier, for which 0.3 m w.e. a $^{-1}$ is assumed. If uncertainty in stake measurements is the same order, and if the two sources are mutually uncorrelated, they combine to 0.4 m w.e. a $^{-1}$.

Reconstructed surface mass balance, $b_{\text{sfc}}(z)$, over 1948–2007 at 1000 m a.s.l. (Fig. 7) has three distinct periods: before, during and after 1970–94. Mean annual balances were $+0.18$, $+0.92$ and -0.86 m w.e. in the three periods (Table 1). Compared with the middle period, the first

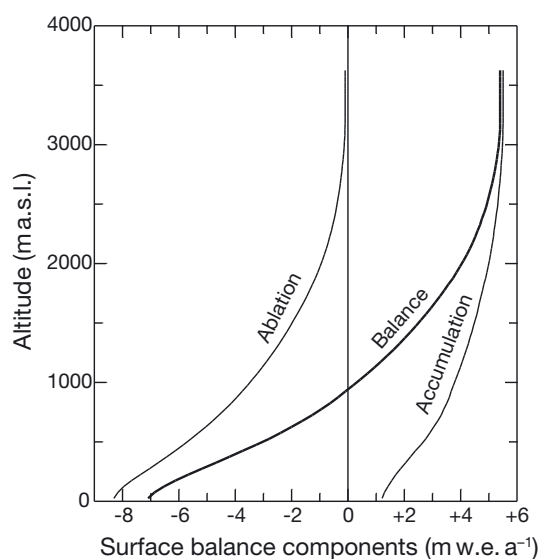


Fig. 6. Altitude variation of mean 1948–2007 surface mass-balance components.

and third were much drier, and the three periods were progressively warmer in winter, with a decreasing fraction of precipitation falling as snow. The role of Figure 7 is to separate effects of changing climate conditions from effects of changing glacier geometry. With surface lowering, for instance, the strong vertical gradients of the three components of surface mass balance (Fig. 6) would cause it to become more negative even if climate were unchanging.

Over June–September at 1000 m a.s.l., 1964–92 was 0.9°C cooler than either the previous or following period. These shifts correspond roughly with rises in North Pacific sea-surface temperature, in winter after 1976 and in summer after 1988 (Hare and Mantua, 2000). The Pacific Decadal Oscillation index was strongly negative in the first period, strongly positive in the middle period and mildly positive in the third.

Seasonal evolution of mean 1948–2007 modeled cumulative surface mass balance is shown for 0, 500, 1000, 1500 and 2000 m a.s.l. in Figure 8. The curves for higher altitudes nearly coincide for the first ~200 days of the season because precipitation is assumed to be constant with altitude, and above ~1500 m a.s.l. temperatures are predominantly $< +2^{\circ}\text{C}$.

Sensitivity of model results to temperature shows that surface ablation at 1000 m a.s.l. would increase by 0.8 m w.e. a⁻¹ under 1°C warming. In addition, change in the rain/snow partitioning would cause surface accumulation to decrease by 0.3 m w.e. a⁻¹ for a total decrease of surface

Table 1. Mean glacier-wide surface mass-balance components at 1000 m a.s.l. over principal subperiods (Fig. 7) calculated with $\phi' = 200^{\circ}$, $\alpha = 0.0061 \text{ s}$ and $\beta = -0.0041 \text{ m w.e. d}^{-1} \text{ }^{\circ}\text{C}^{-1}$

| Variable | 1948–69 | 1970–94 | 1995–2007 |
|--|---------|---------|-----------|
| Accumulation (m w.e. a ⁻¹) | 3.79 | 4.15 | 3.02 |
| Balance (m w.e. a ⁻¹) | 0.18 | 0.92 | -0.86 |
| Ablation (m w.e. a ⁻¹) | -3.62 | -3.23 | -3.88 |

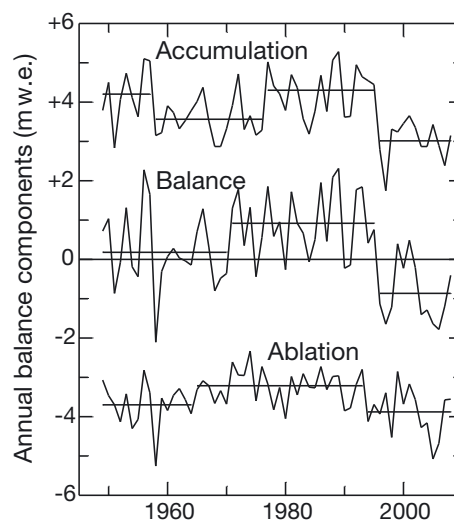


Fig. 7. Mean 1948–2007 October–September surface mass-balance model results (m w.e. a⁻¹) at 1000 m a.s.l. Each series is fit with a piecewise-constant function, stages of which are determined empirically, so the probability, $p\{t\}$, is small, according to the t test, that the values in two successive stages are from the same population. For all pairs of successive stages, $p\{t\} < 0.01$.

mass balance of 1.1 m w.e. a⁻¹. Under an independent 10% increase in precipitation, surface accumulation would increase by 0.42 m w.e. a⁻¹. The effect of possibly increased cloudiness accompanying the increased precipitation on received solar radiation, and hence on surface ablation, is not considered.

Lemke and others (2007) project that by 2100 temperature in the region will increase 3.2°C and precipitation by 21%, which have countervailing effects on surface balance. Combining sensitivities and projections yields changes by 2100 in surface accumulation of -0.1 m w.e. a⁻¹, in surface ablation of -2.6 m w.e. a⁻¹ and in balance of -2.7 m w.e. a⁻¹. Sensitivities and projections are expressed here using the index altitude 1000 m a.s.l. to separate climate effects from possible effects of changing glacier geometry.

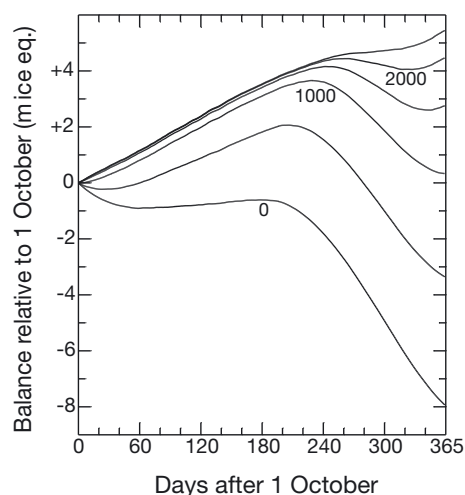


Fig. 8. Mean 1948–2007 seasonal evolution of cumulative surface mass-balance model results relative to 1 October at 0, 500, 1000, 1500, 2000 and 2500 m a.s.l.

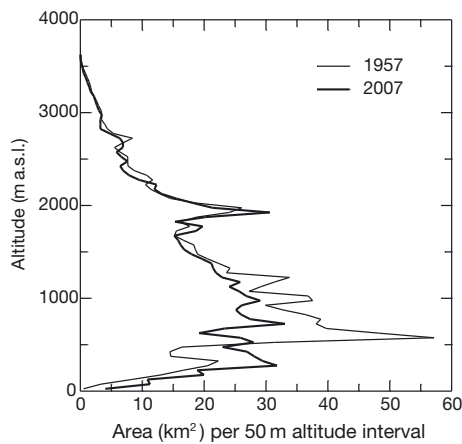


Fig. 9. Area–altitude distributions with $\delta A(z)$ in km^2 per 50 m altitude increments. In 1957 the total area was 1068 km^2 and the mean altitude was 1246 m; in 2007 they were 973 km^2 and 1232 m.

Glacier-wide balances

The integral of surface mass balance over the area–altitude distribution (AAD) (Fig. 9) is approximated by

$$B_{\text{sfc}} = \sum_{i=1}^n \delta A(z_i) b_{\text{sfc}}(z_i), \quad (6)$$

in which $\delta A(z_i)$ is the glacier area in the altitude interval $[z_i - 25 \text{ m}, z_i + 25 \text{ m}]$. The 1957 AAD serves as a useful reference topography, as discussed by Elsberg and others (2001), which is relevant for climate investigations. Integrating over the evolving AAD, by contrast, combines the effects of climate variation and topography variation, which is relevant to investigation of total iceberg production.

Instead of explicitly obtaining intermediate AAD between 1957 and 2007, $B_{\text{sfc}}(t)$ is approximated by interpolating linearly between $B_{\text{sfc}}^{1957}(t)$ and $B_{\text{sfc}}^{2007}(t)$ in proportion to the variation of volume, $V(t)$, relative to the 2007 volume:

$$B_{\text{sfc}}(t) = B_{\text{sfc}}^{2007}(t) + \left[B_{\text{sfc}}^{1957}(t) - B_{\text{sfc}}^{2007}(t) \right] V(t)/V(1957). \quad (7)$$

In the absence of detailed information on the evolution of the topography, the zero-order assumption is made that change in AAD follows change in volume.

The integral over the 1957 AAD exceeds that over the 2007 AAD by $\sim 0.4 \text{ km}^3$ in heavy surface accumulation years and by $\sim 0.1 \text{ km}^3$ in light accumulation years. That is, high accumulation years favored $B_{\text{sfc}}^{1957}(t)$ more than $B_{\text{sfc}}^{2007}(t)$. Correlation of the difference with accumulation is $r = +0.54$, but with surface ablation it is negligible. Variation of $B_{\text{sfc}}(t)$ integrated over the evolving AAD is shown in Figure 10. The generally positive surface mass balance from 1948 to 1995 was caused primarily by high surface accumulation over that period (Fig. 7).

Comparison with other glaciers

There are three glaciers in the region where the USGS has maintained surface mass-balance programs: Wolverine (60.4° N , 148.9° W , since 1966); Gulkana (63.3° N , 145.4° W , since 1966) and South Cascade (48.4° N , 121.1° W , since 1959). Critical direction, ϕ' , assumed by the surface accumulation component, c_{sfc} , of the model (Equations (1) and (2)), for Wolverine Glacier is 122° and

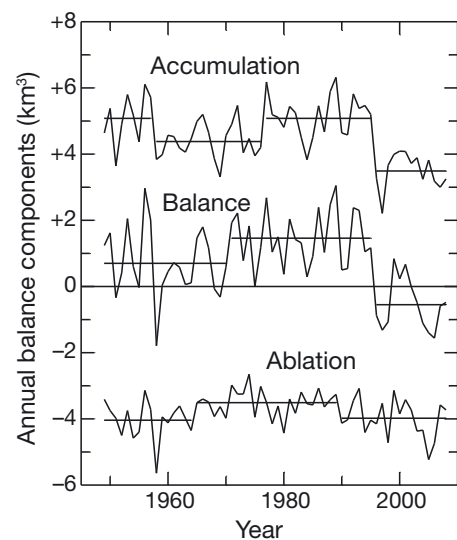


Fig. 10. Annual surface mass-balance model results integrated over evolving topography. Piecewise-constant function as in Figure 7, with $p\{t\} \leq 0.01$ for all pairs of successive stages.

for Gulkana Glacier is 238° (Rasmussen and Conway, 2004), compared with 200° for Columbia Glacier.

Calculated glacier-wide annual surface accumulation, C_{sfc} , at Columbia Glacier (Equations (1) and (6)) correlated with glacier-wide winter balance, B_w , positively at Wolverine Glacier ($r = +0.37$), but negligibly at South Cascade and Gulkana Glaciers. Calculated glacier-wide annual surface ablation, A_{sfc} , (Equations (3) and (6)) correlated strongly with glacier-wide summer balance, B_s , at Wolverine ($+0.80$) and Gulkana ($+0.76$) Glaciers, but negligibly at South Cascade Glacier. Reference-surface balances (Elsberg and others, 2001) are used for all glaciers to take out the effects of changing glacier geometry.

VOLUME CHANGE AND ICEBERG PRODUCTION

Glacier volume change

Glacier topography is summarized concisely by its area–altitude distribution, shown in Figure 9 for 1957 and 2007. Change of glacier volume above sea level, $\Delta V^+ = -131 \text{ km}^3$, over 1957–2007 is calculated geodetically using the two AADs. For comparison, E. Berthier (personal communication, 2010) estimated a loss of volume above sea level of $136 \pm 5 \text{ km}^3$. Dynamic thinning and disintegration of the lower reach between the pre-retreat position of the terminus, $L = 67 \text{ km}$, and its 2007 position, $L = 50 \text{ km}$, (Fig. 1) has been the major source of icebergs.

Effects of tectonic uplift are neglected. Plafker (1969) analyzed changes after the 27 March 1964 magnitude 8.4 earthquake with epicenter 61.06° N , 147.44° W . Although changes in the region varied from -2.5 to $+11.5 \text{ m}$, they were negligible at Columbia Glacier and were -0.3 m at Valdez.

Changes in the mass of firn are also neglected by assuming Sorge's law (Bader, 1954). This holds that the density profile from the surface to the firn/ice transition is unchanging, so the entire thickness change in the ice/firn/snow column is due to change in the thickness of the ice. Since rapid retreat began, the total thickness has changed by hundreds of meters

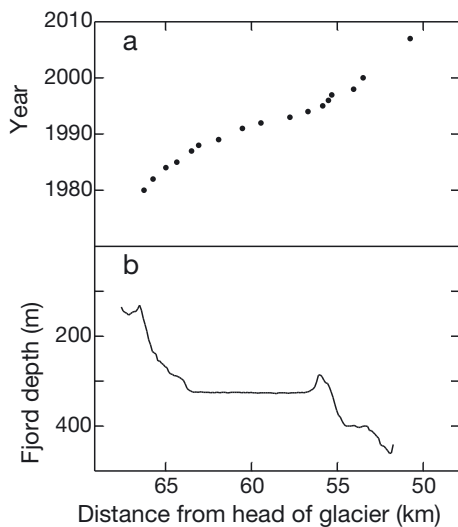


Fig. 11. (a) Terminus-retreat history (Krimmel, 2001) and (b) maximum depth in 2005 bathymetric survey along east-west line at each distance, L , from head of the glacier.

(Walter and others, 2010), so the possible changes in the firm thickness are comparatively small.

On the assumption that glacier topography changed little between 1948 and 1957, the total 1948–2007 volume change is taken to be the same as the total 1957–2007 change. When the USGS began ground observations in the mid-1970s, the basin seemed to be full of ice; i.e. ice levels from the terminus to the equilibrium line were abutting, but not encroaching into, mature heather and other plants growing in several inches of soil. This and old photographs by E.H. Harriman and W.O. Field (Brown, 2004) suggest that the glacier had been stable for several decades prior to then.

Estimating 1948–2007 change of glacier volume below sea level, ΔV^- , is less certain. A bathymetric survey conducted by the NOAA in September 2005 sounded the full width of the fjord that had been previously occupied by the glacier as far north as $L = 57.4$ km (Fig. 1), yielding a volume of 10.6 km³. Between there and $L = 52.1$ km, the northern extent of the survey, floating ice prevented sounding the full width of the fjord. At each L value, on each side of the fjord, linear extrapolation from the last depth sounded to zero at the margin of the fjord yields an additional volume of 0.3 km³.

Maximum depth from the 2005 survey along an east-west line at each distance, L , from the head of the glacier is shown in Figure 11, along with the terminus-retreat history from figure 14 of Krimmel (2001). The volume between $L = 52.1$ km and the 2007 terminus, $L = 50$ km, is roughly estimated as an additional ~ 2 km³. In sum, these yield $\Delta V^- \approx -13$ km³. When combined with the value $\Delta V^+ = -131$ km³, the total volume change is $\Delta V \approx -144$ km³.

Comparison of the 2005 bathymetry with soundings made in the mid-1990s (Krimmel, 2001) showed that the 2005 depths were ~ 7 m shallower over the section of the fjord between $L = 55$ and 67 km. In the case of erosion, Motyka and others (2006) found during advance of Taku Glacier, Alaska, that rates averaged 4 m a⁻¹ over 1989–2003. Uncertainty in the possible changes in the fjord bed is much smaller than the mean depth, which is ~ 300 m.

There are three principal sources of uncertainty in the 1948–2007 volume change, ΔV . The largest is that in the change above sea level, ΔV^+ , for which Berthier's 5 km³

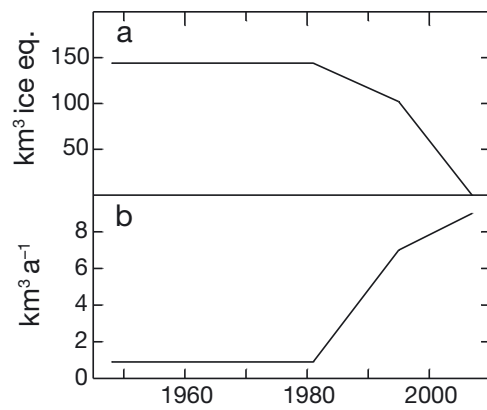


Fig. 12. (a) Evolution of volume, $V(t)$, relative to 2007 and (b) piecewise-linear calving rate, $dD(t)/dt$, consistent with it and with the 1981–95 variation of Krimmel (2001). Over 1948–81, $dD(t)/dt$ is shown as a uniform value integrating to $\sum D = \sum B_{sfc}$ over that period (Table 2).

is assumed. Next largest is that in the -13 km³ change below sea level, ΔV^- , calculated from the 2005 NOAA bathymetry, which is assumed to be 2 km³. Third is possible change in the bathymetry due to sediment transport between the onset of retreat and 2005, for which 1 km³ is assumed. On the further assumption that these three are mutually uncorrelated, the resultant uncertainty is 5.5 km³.

Total iceberg production

Where ΔV is the change of volume, $\sum B_{sfc}$ the sum of annual $B_{sfc}(t)$ and $\sum D$ the sum of annual calving volumes over any period of years, the three quantities are related through

$$\sum D = \sum B_{sfc} - \Delta V. \quad (8)$$

Observations discussed above indicate that the glacier volume changed little from 1948 to 1981, but decreased ~ 144 km³ from 1981 to 2007. That is, the amount, $V(t)$, by which the volume exceeded the 2007 volume was ~ 144 km³ from 1948 to 1981. Annual $B_{sfc}(t)$ summed over the 15 years from 1981 to 1995 (Equation (6)) gives $\sum B_{sfc} = 18$ km³ ice eq. Krimmel (2001, fig. 20) shows that over 1981–95 the calving flux, dD/dt , increased roughly linearly from ~ 1.5 km³ a⁻¹ in 1981 to ~ 7 km³ a⁻¹ in 1995; total calving volume, $\sum D$, over that period was 60 km³.

Evolution of the volume thus assumed is shown in Figure 12, along with a piecewise-linear calving rate, $dD(t)/dt$, consistent with it and with the 1981–95 variation of Krimmel (2001); over 1995–2007 $dD(t)/dt$ varied linearly from 7 km³ a⁻¹ in 1995 to 9 km³ a⁻¹ in 2007. Values of ΔV , $\sum B_{sfc}$ and $\sum D$ are shown in Table 2 for each of the three subperiods. The 1948–2007 $\sum B_{sfc}$ is 42 km³ ice eq., which combined with the ~ 144 km³ volume loss yields a total iceberg volume of ~ 186 km³. The cause of the difference in slope of $dD(t)/dt$ between 1981–95 and 1995–2007 (Fig. 12) is that $\sum B_{sfc}$ over the first subperiod is $+18$ km³ ice eq. and over the second is -6 km³ ice eq. That is, over the first subperiod $\sum B_{sfc} > 0$ augmented $\Delta V < 0$ in producing $\sum D$ (Equation (8)), whereas in the second subperiod part of the $\Delta V < 0$ was caused by $\sum B_{sfc} < 0$. About 64% of the decline in $\sum B_{sfc}$ between the two subperiods was due to reduced surface accumulation, caused by both warming and drying, and the rest was due to increased surface ablation.

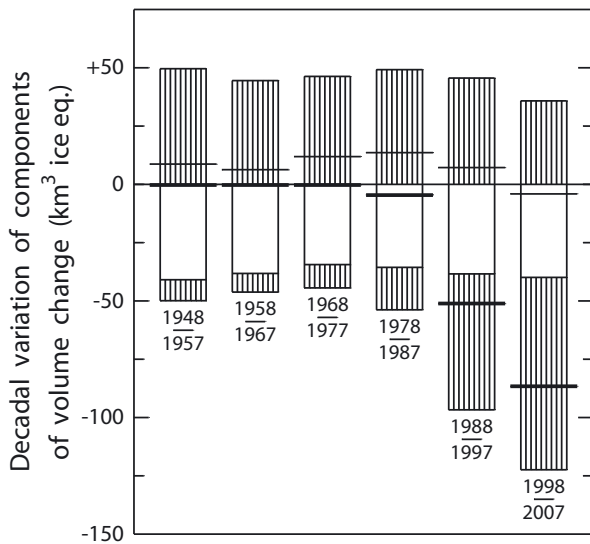


Fig. 13. Decadal variation of components of volume change. Upper striped bar: glacier-wide surface accumulation; open bar: glacier-wide surface ablation; lower striped bar: calving; upper horizontal line: net glacier-wide surface mass balance; lower horizontal line: total volume change. Because of lack of detailed information on the evolution, $V(t)$, of the volume of the glacier, the calving rate, dD/dt , is not strictly constant over 1948–81 but averages the same value as in Figure 12 ($0.9 \text{ km}^3 \text{ a}^{-1}$), so that volume change then is nearly zero.

From 1948 until drastic retreat began, ~ 1981 , when volume change of the glacier was small, almost all iceberg production (30 km^3) was from positive surface mass balance (Fig. 13). More detailed analysis of changes in calving is not possible because of uncertainties in the evolution of the volume of the glacier. Moreover, without using an advanced dynamic model it is not possible to determine the trajectories down to the calving front of changes in surface mass balance over the extent of the glacier.

Surface mass balance during the 1960s, for example, was slightly positive (Fig. 10). From continuity (Equation (8)), calving over that decade would also have been small, unless the glacier volume was decreasing. In addition, observations during the 1970s by Meier and others (1978) indicated up to 10 m a^{-1} of localized thinning near the terminus and increased iceberg discharge. During retreat, from 1981 to 2007, surface mass balance ($12 \text{ km}^3 \text{ ice eq.}$) contributed only 8% of the total iceberg production (156 km^3). The remainder was from dynamic thinning and disintegration of the part of the lower reach between the pre-retreat terminus and the 2007 terminus.

DISCUSSION

Use of upper-air meteorological data in the NCEP/NCAR Reanalysis database has several advantages over using data from weather service stations or from instruments installed on or near the glacier. The temporal resolution and continuity of the record since 1948 make it a valuable resource for surface mass-balance modeling. The model described here can therefore compute surface mass balance over any time interval at any altitude.

The model adopts two simplifications that differ from assumptions usually made in mass-balance modeling, but that are justified by results here. One is that precipitation is constant with altitude. At Columbia Glacier, altitude increases generally to the north, away from the coast, which is in the downwind direction during precipitation events. Whereas precipitation might increase with altitude locally, it also decreases with distance from the coast, along the maritime/continental gradient in the region. Surface accumulation in the model does increase with altitude, even though precipitation does not because temperature decreases with altitude, so the fraction of precipitation falling as snow increases.

Another atypical model result is that the degree-day factor, β , can be constant with altitude. Its value is typical of values found in numerous PDD models for surface ablation on other glaciers (e.g. Braithwaite and Zhang, 2000; Hock, 2003), although in those models a larger value is used for exposed ice than for a snow-covered surface. The lower-albedo ice surface is exposed for a longer summer period at low altitude than at high, thus enhancing absorption of solar radiation over the season. Another condition at some glaciers is that their lower reaches are shaded for part of the day by nearby topography whereas the higher reaches are not. Because Columbia Glacier is large with little nearby strong relief except to the north, this effect is small there.

Although both simplifications would seem to contribute to negative model bias at higher altitude (underestimating surface accumulation and overestimating the magnitude of surface ablation) and the opposite bias at lower altitude, they are justified by the fact that model error, $b_{\text{sfc}} - \hat{b}_{\text{sfc}}$, is uncorrelated with altitude ($r = +0.05$). Much model error comes from the assumption that mass-balance components do not vary along an altitude contour. Measurements vary principally with altitude but there is a slight secondary variation, such as in the values at $\sim 500 \text{ m}$ (Fig. 5). The model's inability to capture any lateral variation is a source of much of its error, but failing to capture variation with altitude is not.

In this work we cannot speculate on future dynamic behavior of the glacier, but results do provide a basis

Table 2. Variation of volume, V , annual surface mass balance, B_{sfc} , surface accumulation, C_{sfc} , surface ablation, A_{sfc} , and calving, D , over principal periods of glacier change (Equation (8))

| Period | Total | | | Rate | | | | |
|-----------|---------------------------------------|--|-------------------------------------|--|---|---|---|--|
| | ΔV km ³ ice eq. | $\sum B_{\text{sfc}}$ km ³ ice eq. | $\sum D$ km ³ ice eq. | dV/dt km ³ ice eq. a ⁻¹ | B_{sfc} km ³ ice eq. a ⁻¹ | C_{sfc} km ³ ice eq. a ⁻¹ | A_{sfc} km ³ ice eq. a ⁻¹ | dD/dt km ³ ice eq. a ⁻¹ |
| 1948–81 | 0 | 30 | 30 | 0.0 | 0.9 | 4.4 | –3.5 | 0.9 |
| 1982–95 | –42 | 18 | 60 | –3.0 | 1.3 | 4.7 | –3.4 | 4.3 |
| 1996–2007 | –102 | –6 | 96 | –8.5 | –0.5 | 3.5 | –4.0 | 8.0 |
| 1948–2007 | –144 | 42 | 186 | –2.4 | 0.7 | 4.3 | –3.6 | 3.1 |

for estimating thinning due to surface mass-balance processes. The approximately $-0.5 \text{ km}^3 \text{ ice eq. a}^{-1}$ surface mass balance over 1995–2007 (Fig. 10) when distributed across the $\sim 970 \text{ km}^2$ area of the glacier averages $\sim 0.5 \text{ m a}^{-1}$ thinning. Finer temporal resolution of the volume change and calving rate requires more advanced dynamic models (e.g. Pfeffer, 2007; Otero and others, 2010).

The finding that the retreat phase of Columbia Glacier proceeds independently of climate is not new (Clarke, 1987; Meier and Post, 1987; O'Neel and others, 2005; Pfeffer, 2007). Such fast dynamic behavior is not restricted to tidewater glaciers of Alaska but is also a feature of outlet glaciers in Antarctica (Rignot and others, 2008) and Greenland (Howat and others, 2007; Joughin and others, 2010). Additional studies are needed to quantify the processes and timescales that control the dynamic responses, and also to assess fluxes of surface mass balance and calving at other tidewater glacier systems.

CONCLUSIONS

Models of surface mass balance together with volume-change calculations are needed to determine the total volume of iceberg discharge from tidewater glaciers. Prior to retreat of Columbia Glacier, positive surface mass balance was offset by an equal amount of iceberg production (30 km^3), an inference that was a direct consequence of assuming that the glacier volume was unchanging then. Calving then was only about a quarter of surface ablation (i.e. $\sim 4 \text{ km}^3 \text{ ice eq. a}^{-1}$) and changed little over 1948–2007.

Between 1981 and 2007 the glacier experienced a period of accelerating volume decrease, mainly due to an increasing rate of iceberg production. During the first half of the retreat (1982–95), $4.3 \text{ km}^3 \text{ a}^{-1}$ of ice was lost due to iceberg calving. This loss was partly offset by a $1.3 \text{ km}^3 \text{ a}^{-1}$ gain in volume from positive surface mass balance over this period. In the later part of the retreat (1996–2007), $8.0 \text{ km}^3 \text{ a}^{-1}$ of ice was lost by iceberg calving, with an additional $0.5 \text{ km}^3 \text{ a}^{-1}$ of ice loss due to negative surface mass balance. Over 1948–81, calving was due entirely to positive surface mass balance, whereas since then only 8% has been, 92% being due to volume loss of the glacier (Table 2).

Allocating 1948–2007 calving volume, $\sum D \approx 186 \text{ km}^3$, to sea-level rise depends on the timescale considered. Over the period since retreat began, the biggest part is due to change, $\Delta V^+ \approx -131 \text{ km}^3$, of the volume above sea level. Some of the $\sum B_{\text{sic}} \approx 42 \text{ km}^3 \text{ ice eq.}$ contribution from surface mass balance includes short-term recycling of water from the sea. Results (Table 2) indicate that the contribution to sea-level rise increased from $\sim 0.008 \text{ mm a}^{-1}$ during 1982–95 to $\sim 0.023 \text{ mm a}^{-1}$ during 1996–2007 (determined using $3.62 \times 10^8 \text{ km}^2$ as the area of the sea). The recent value is slightly more than 1% of the total present-day eustatic sea-level rise of $\sim 1.8 \text{ mm a}^{-1}$ estimated by Meier and others (2007). Loss of volume below sea level, $\Delta V^- \approx -13 \text{ km}^3$, did not contribute because it was already displacing sea water. Moreover, as a consequence of the density difference between ice and sea water, its melting would slightly lower sea level.

ACKNOWLEDGEMENTS

We thank S. O'Neel for supplying the 2005 bathymetric survey and the area–altitude distribution for 1957, E. Berthier

for the 2007 distribution, R. March for securing the base map for Figure 1 and H. Greenberg for determining the 2007 terminus position. Comments by W.T. Pfeffer improved the scope and content of the paper. Thoughtful comments by two anonymous reviewers greatly improved the clarity of the paper and are deeply appreciated. This work was supported by US National Science Foundation grant ARC 0732739.

REFERENCES

- Andreassen, L.M. and J. Oerlemans. 2009. Modelling long-term summer and winter balances and the climate sensitivity of Storbreven, Norway. *Geogr. Ann.*, **91**(4), 233–251.
- Arendt, A.A., K.A. Echelmeyer, W.D. Harrison, C.S. Lingle and V.B. Valentine. 2002. Rapid wastage of Alaska glaciers and their contribution to rising sea level. *Science*, **297**(5580), 382–386.
- Bader, H. 1954. Sorge's Law of densification of snow on high polar glaciers. *J. Glaciol.*, **2**(15), 319–323.
- Berthier, E., E. Schiefer, G.K.C. Clarke, B. Menounos and F. Rémy. 2010. Contribution of Alaskan glaciers to sea-level rise derived from satellite imagery. *Nature Geosci.*, **3**(2), 92–95.
- Bevington, P.R. 1969. *Data reduction and error analysis for the physical sciences*. New York, McGraw-Hill.
- Braithwaite, R.J. and Y. Zhang. 2000. Sensitivity of mass balance of five Swiss glaciers to temperature changes assessed by tuning a degree-day model. *J. Glaciol.*, **46**(152), 7–14.
- Brown, C.S. 2004. *With a camera in my hands: William O. Field, pioneer glaciologist*. Fairbanks, AK, University of Alaska Press.
- Calkin, P.E., G.C. Wiles and D.J. Barclay. 2001. Holocene coastal glaciation of Alaska. *Quat. Sci. Rev.*, **20**(1–3), 449–461.
- Clarke, G.K.C. 1987. Fast glacier flow: ice streams, surging and tidewater glaciers. *J. Geophys. Res.*, **92**(B9), 8835–8841.
- De Woul, M. and R. Hock. 2005. Static mass-balance sensitivity of Arctic glaciers and ice caps using a degree-day approach. *Ann. Glaciol.*, **42**, 217–224.
- Elsberg, D.H., W.D. Harrison, K.A. Echelmeyer and R.M. Krimmel. 2001. Quantifying the effects of climate and surface change on glacier mass balance. *J. Glaciol.*, **47**(159), 649–658.
- Førland, E.J. and I. Hanssen-Bauer. 2003. Past and future climate variations in the Norwegian arctic: overview and novel analysis. *Polar Res.*, **22**(2), 113–124.
- Hare, S.R. and N.J. Mantua. 2000. Empirical evidence for North Pacific regime shifts in 1977 and 1989. *Progr. Oceanogr.*, **47**(2–4), 103–145.
- Hock, R. 2003. Temperature index melt modelling in mountain areas. *J. Hydrol.*, **282**(1–4), 104–115.
- Howat, I.M., I.R. Joughin and T.A. Scambos. 2007. Rapid changes in ice discharge from Greenland outlet glaciers. *Science*, **315**(5818), 1559–1561.
- Joughin, I., B.E. Smith, I.M. Howat, T. Scambos and T. Moon. 2010. Greenland flow variability from ice-sheet-wide velocity mapping. *J. Glaciol.*, **56**(197), 415–430.
- Kalnay, E. and 21 others. 1996. The NCEP/NCAR 40-year reanalysis project. *Bull. Am. Meteorol. Soc.*, **77**(3), 437–471.
- Kistler, R. and 12 others. 2001. The NCEP/NCAR 50-year reanalysis: monthly means CD-ROM and documentation. *Bull. Am. Meteorol. Soc.*, **82**(2), 247–267.
- Kohler, J. and R. Aanes. 2004. Effect of winter snow and ground-icing on a Svalbard reindeer population: results of a simple snowpack model. *Arct. Antarct. Alp. Res.*, **36**(3), 333–341.
- Korona, J., E. Berthier, M. Bernard, F. Rémy and E. Thouvenot. 2009. SPIRIT. SPOT 5 stereoscopic survey of Polar Ice: Reference Images and Topographies during the fourth International Polar Year (2007–2009). *ISPRS J. Photogramm. Rem. Sens.*, **64**(2), 204–212.
- Krimmel, R.M. 2001. Photogrammetric data set, 1957–2000, and bathymetric measurements for Columbia Glacier, Alaska. *USGS Water-Resour. Invest. Rep.* 01-4089.

- Lemke, P. and 10 others. 2007. Observations: changes in snow, ice and frozen ground. In Solomon, S. and 7 others, eds. *Climate change 2007: the physical science basis. Contribution of Working Group I to the Fourth Assessment Report of the Intergovernmental Panel on Climate Change*. Cambridge, etc., Cambridge University Press, 339–383.
- Mayo, L.R., D.C. Trabant, R. March and W. Haeberli. 1979. Columbia Glacier stake location, mass balance, glacier surface altitude, and ice radar data: 1978 measurement year. *USGS Open File Rep.* 79-1168.
- Meier, M.F. and A. Post. 1987. Fast tidewater glaciers. *J. Geophys. Res.*, **92**(B9), 9051–9058.
- Meier, M.F. and 10 others. 1978. Columbia Glacier progress report: December 1977. *USGS Open File Rep.* 78-264.
- Meier, M.F. and 7 others. 2007. Glaciers dominate eustatic sea-level rise in the 21st century. *Science*, **317**(5841), 1064–1067.
- Motyka, R.J., M. Truffer, E.M. Krüger and A.K. Bucki. 2006. Rapid erosion of soft sediments by tidewater glacier advance: Taku Glacier, Alaska, USA. *Geophys. Res. Lett.*, **33**(24), L24504. (10.1029/2006GL028467.)
- O'Neel, S., W.T. Pfeffer, R. Krimmel and M. Meier. 2005. Evolving force balance at Columbia Glacier, Alaska, during its rapid retreat. *J. Geophys. Res.*, **110**(F3), F03012. (10.1029/2005JF000292.)
- Oerlemans, J. 1991. A model for the surface balance of ice masses: Part 1. Alpine glaciers. *Z. Gletscherkd. Glazialgeol.*, **27/28**, 63–83.
- Otero, J., F.J. Navarro, C. Martín, M.L. Cuadrado and M.I. Corcuera. 2010. A three-dimensional calving model: numerical experiments on Johnsons Glacier, Livingston Island, Antarctica. *J. Glaciol.*, **56**(196), 200–214.
- Pfeffer, W.T. 2007. A simple mechanism for irreversible tidewater glacier retreat. *J. Geophys. Res.*, **112**(F3), F03S25. (10.1029/2006JF000590.)
- Plafker, G. 1969. Tectonics of the March 27, 1964, Alaska earthquake. *USGS Prof. Pap.* 543-I.
- Post, A. 1975. Preliminary hydrography and historic terminal changes of Columbia Glacier, Alaska. *USGS Hydrol. Invest. Atlas* HA-559.
- Rasmussen, L.A. 2005. Mass balance of Vatnajökull outlet glaciers reconstructed back to 1958. *Jökull*, **55**, 139–146.
- Rasmussen, L.A. 2009. South Cascade Glacier mass balance, 1935–2006. *Ann. Glaciol.*, **50**(50), 215–220.
- Rasmussen, L.A. and H. Conway. 2001. Estimating South Cascade Glacier (Washington, USA) mass balance from a distant radiosonde and comparison with Blue Glacier. *J. Glaciol.*, **47**(159), 579–588.
- Rasmussen, L.A. and H. Conway. 2003. Using upper-air conditions to estimate South Cascade Glacier (Washington, USA) summer balance. *J. Glaciol.*, **49**(166), 456–462.
- Rasmussen, L.A. and H. Conway. 2004. Climate and glacier variability in western North America. *J. Climate*, **17**(9), 1804–1815.
- Rasmussen, L.A. and H. Conway. 2005. Influence of upper-air conditions on glaciers in Scandinavia. *Ann. Glaciol.*, **42**, 402–408.
- Rasmussen, L.A. and J. Kohler. 2007. Mass balance of three Svalbard glaciers reconstructed back to 1948. *Polar Res.*, **26**(2), 168–174.
- Rasmussen, L.A. and J.M. Wenger. 2009. Upper-air model of summer balance on Mount Rainier, USA. *J. Glaciol.*, **55**(192), 619–624.
- Rignot, E. and 6 others. 2008. Recent Antarctic ice mass loss from radar interferometry and regional climate modelling. *Nature Geosci.*, **1**(2), 106–110.
- Schneider, S.H. and 10 others. 2007. Assessing key vulnerabilities and the risk from climate change. In Parry, M.L., O.F. Canziani, J.P. Palutikof, P.J. van der Linden and C.E. Hanson, eds. *Climate change 2007: impacts, adaptation and vulnerability. Contribution of Working Group II to the Fourth Assessment Report of the Intergovernmental Panel on Climate Change*. Cambridge, etc., Cambridge University Press, 799–810.
- Van Beusekom, A.E., S.R. O'Neel, R.S. March, L.C. Sass and L.H. Cox. 2011. Re-analysis of Alaskan benchmark glacier mass-balance data using the index method. *USGS Sci. Invest. Rep.* 2010-5247.
- Van der Veen, C.J. 1995. Controls on calving rate and basal sliding: observations from Columbia Glacier, Alaska, prior to and during its rapid retreat, 1976–1993. *Byrd Polar Res. Cent. Rep.* 11.
- Vancouver, G. 1798. *A voyage of discovery to the North Pacific Ocean, and round the World; in which the coast of North-west America has been carefully examined and accurately surveyed. 1790–1795, Vol. 3*. London, G.G. and J. Robinson and J. Edwards.
- Walter, F., S. O'Neel, D.E. McNamara, T. Pfeffer, J. Bassis and H.A. Fricker. 2010. Iceberg calving during transition from grounded to floating ice: Columbia Glacier, Alaska. *Geophys. Res. Lett.*, **37**(15), L15501. (10.1029/2010GL043201.)

MS received 9 July 2010 and accepted in revised form 30 January 2011